*Techniques in Mathematics, Physics and Engineering* (Holt, Rinehart and Winston, Inc., New York, 1964); (b) W. F. Ames, *Nonlinear Ordinary Differential Equations in Transport Processes* (Academic Press Inc., New York, 1968); (c) *Differential Equations and Dynamical Systems*, J. K. Hale and J. P. LaSalle, Eds. (Academic Press Inc., New York, 1967).

[6] R. A. Marcus, J. Chem. Phys. (to be published).

[7] Compare A. O. Cohen and R. A. Marcus, J. Chem. Phys. **49,** 4509 (1968).

[8] E.g., W. Grobner, *Die Lie-Reihen und Ihre Anwendungen* (VEB Deutscher Verlag der Wissenschaften, Berlin, 1967), 2nd ed. (autonomous systems); cf. K. T. Chen, Arch. Rat. Mech. Anal. **13,** 348 (1963), which came to our attention after submission of the present article. It contains a quite different derivation of (11), lengthier than the present though self-contained.

[9] W. Magnus, Commun. Pure Appl. Math. **7,** 649 (1954).

[10] For example when (1) represents a system of equations of classical mechanical motion for a collision of two particles, $h_i^1$ reflects their interaction. In a conservative system neither $h_i^0$ nor $h_i^1$ depend explicitly on time $t$, but nevertheless $h_i^1$ vanishes as $t \to \pm\infty$, because in the usual collision problems the particles are then far apart. ($t_0$ is chosen to be any arbitrary time in the region where the initial interaction of the particles is negligible.)

[11] W. Grobner, Ref. 8, p. 17.

[12] In a related problem, coefficients of the Baker–Campbell–Hausdorff series have been calculated to a high order by computer [R. D. Richtmyer and S. Greenspan, Commun. Pure Appl. Math. **18,** 107 (1965).] Applications of Magnus' solution are given in D. W. Robinson, Helv. Phys. Acta **36,** 140 (1963); P. Pechukas and J. C. Light, J. Chem. Phys. **44,** 3897 (1966); S. Chan, J. C. Light and J. Lin, *ibid.* **49,** 86 (1968); E. H. Wichmann, J. Math. Phys. **2,** 876 (1961); R. M. Wilcox, *ibid.* **8,** 962 (1967) and references cited therein; M. Lutzky, *ibid.* **9,** 1125 (1968). Sometimes the third term of the series is written more symmetrically, but the present form, due to Magnus, emphasizes that the series terminates if $A_{ti}$ and

$$\int_{t_0}^{t_i} A_{ti} dt_j$$

commute.

[13] E. H. Abate and F. Hofelich, Z. Physik **209,** 13 (1968).

[14] (a) L. M. Garrido, Proc. Phys. Soc. (London) **76,** 33 (1960); J. Math. Anal. Appl. **3,** 295 (1961); (b) L. M. Garrido and F. Gascon, Proc. Roy. Soc. (London) **81,** 1115 (1963).

[15] See, e.g., K. T. Chen, Ref. 8; J. Diff. Equations **2,** 438 (1966); for classical mechanics see L. M. Garrido and F. Gascon, Ref. 14, Eq. 12, a result discussed later.

[16] (a) For example E. Merzbacher, *Quantum Mechanics* (John Wiley & Sons, Inc., New York, 1961), p. 464. (b) Thus, as seen from (21) $D$ now becomes for the system (20), the "Liouville operator," defined, for example, in R. W. Zwanzig, in *Lectures in Theoretical Physics*, W. E. Brittin, B. W. Downs and J. Downs, Eds. (Interscience Publishers, Inc., New York, 1961), p. 107.

[17] (a) See, e.g., H. C. Corben and P. Stehle, *Classical Mechanics* (John Wiley & Sons, Inc., New York, 1960), 2nd ed., pp. 178, 184; (b) E. W. Brown and C. A. Shook, *Planetary Theory* (Cambridge University Press, London, 1933), p. 125.

[18] Reference 17(a), p. 221.

[19] See, e.g., T. E. Sterne, *An Introduction to Celestial Mechanics* (Interscience Publishers, Inc., New York, 1960), p. 100ff; S. W. Groesberg, *Advanced Mechanics* (John Wiley & Sons, Inc., New York, 1968), p. 306ff.

[20] Since the $c_i^0$ are functions of the $q^0$'s and $p^0$'s, (24) and (26) yield $c_i$ equal to $\exp\{B, \quad\} c_i^0$. Finally, the chain rule for differentiation converts $\{B, \quad\}$ to $\sum_{k,j} \{c_k^0, c_j^0\} (\partial B/\partial c_k^0)(\partial/c_j^0)$.

[21] Nonautonomous systems were considered by adjoining $t$ to the set of dependent variables. [See, however, G. R. Sell, in Ref. 5(c), p. 531.] In our case the use of this device would have destroyed the similarity of classical and (the customary) quantum equations used elsewhere in applications.

[22] See, e.g., R. Hermann, *Differential Geometry and the Calculus of Variations* (Academic Press Inc., New York, 1968), Chap. 6; E. L. Ince, *Ordinary Differential Equations* (Dover Publications, Inc., New York, 1956), Chap. IV.

[23] B. O. Koopman, Proc. Nat. Acad. Sci. **17,** 315 (1931); cf. J. von Neumann, Ann. Math. **33,** 587 (1932); E. H. Wichmann, Ref. 12.

[24] Reference 14(b), Eq. (5).

[25] Compare assumption of Eqs. (6) and (7) in Ref. 14(b) whose analog in our case would be our ansatz (6), leading to the automorphism represented by our (9).

[26] Analogy was made by comparison of Eq. (3) of Ref. 14(b) with the "operator equation" there, Eq. (2).

[27] See also Ref. 6, which treats what we have termed there the "interaction" and "mixed-interaction" pictures (or representations) in classical mechanics. In Ref. 14 the first is used, while in the present paper the second is employed, it being the standard one in classical mechanics. Both pictures are treated and compared in Ref. 6.

[28] F. J. Zeleznik, J. Chem. Phys. **47,** 3410 (1967).

[29] Reference 5(a), p. 57.

[30] See, e.g., D. Ter Haar, *Elements of Hamiltonian Mechanics* (North-Holland Publishing Company, Amsterdam, 1961), p. 153; Ref. 17(a), p. 251ff.

THE JOURNAL OF CHEMICAL PHYSICS VOLUME 52, NUMBER 9 1 MAY 1970

# Calculation of Transition Probabilities for Collinear Atom–Diatom and Diatom–Diatom Collisions with Lennard-Jones Interaction

VINCENT P. GUTSCHICK* AND VINCENT MCKOY
*Arthur Amos Noyes Laboratory of Chemical Physics, California Institute of Technology,† Pasadena, California 91109*
AND
DENNIS J. DIESTLER
*Department of Chemistry, University of Missouri,‡ St. Louis, Missouri 63121*

(Received 10 March 1969)

Numerical integration of the close coupled scattering equations is performed to obtain vibrational transition probabilities for three models of the electronically adiabatic $H_2$–$H_2$ collision. All three models use a Lennard-Jones interaction potential between the nearest atoms in the collision partners. The results are analyzed for some insight into the vibrational excitation process, including the effects of anharmonicities in the molecular vibration and of the internal structure (or lack of it) in one of the molecules. Conclusions are drawn on the value of similar model calculations. Among them is the conclusion that the replacement of earlier and simpler models of the interaction potential by the Lennard-Jones potential adds very little realism for all the complication it introduces.

## INTRODUCTION

There is current interest in quantum-mechanical treatments of molecular collisions involving excitation of internal degrees of freedom and possibly reaction. The collision systems pose a multichannel scattering problem, commonly solved by the coupled channels (CC) method. The CC equations are coupled differen-

tial equations derived as follows for a nonreactive system: consider a system composed of two asymptotically isolated parts described by internal coordinates $\mathbf{r}_1$, $\mathbf{r}_2$. Let the relative coordinate be given by $\mathbf{R}$. Into the Schrödinger equation,

$$[T(\mathbf{R})+H^0(\mathbf{r}_1,\mathbf{r}_2)+V_I(\mathbf{r}_1,\mathbf{r}_2,\mathbf{R})-E]\psi(\mathbf{r}_1,\mathbf{r}_2,\mathbf{R})=0 \tag{1}$$

(where $T$ is the operator for kinetic energy of relative motion), substitute the state or channel expansion

$$\psi(\mathbf{r}_1,\mathbf{r}_2,\mathbf{R})=\sum_n f_n(\mathbf{R})\phi_n(\mathbf{r}_1,\mathbf{r}_2), \tag{2}$$

where $\{\phi_n\}$ is a complete orthonormal set of the eigenfunctions of $H_0$,

$$H^0\phi_n=\epsilon_n\phi_n. \tag{3}$$

Left multiplication of Eq. (1) by $\phi_m^*$ and integration over the coordinates $\mathbf{r}_1$, $\mathbf{r}_2$ yields the CC equations

$$(-T(\mathbf{R})+E-\epsilon_m)f_m(\mathbf{R})=\sum_n V_{mn}(\mathbf{R})f_n(\mathbf{R}), \tag{4}$$

where

$$V_{mn}(\mathbf{R})=\langle\phi_m(\mathbf{r}_1,\mathbf{r}_2)\mid V_I(\mathbf{r}_1,\mathbf{r}_2,\mathbf{R})\mid\phi_n(\mathbf{r}_1,\mathbf{r}_2)\rangle. \tag{5}$$

These equations are solved subject to boundary conditions, generally that asymptotically ($|\mathbf{R}|\to\infty$) the relative motion becomes free, i.e.,

$$f_n(\mathbf{R})\sim\exp(i\mathbf{k}_n\cdot\mathbf{R})+\text{scattered waves}. \tag{6}$$

The form of the scattered waves depends upon the dimensionality of the system. The ratio of scattered to incident flux, with flux defined by

$$\mathbf{j}_n(\mathbf{R})=(\hbar/2\mathrm{m})\ \mathrm{Im}(f_n^*\nabla f_n), \tag{7}$$

is the transition probability (one dimension) or cross section (two or three dimensions). As closed-form analytical solutions of Eqs. (4) are not ordinarily obtainable, several techniques have been developed for their accurate numerical integration.[1–5] We developed our own technique of integration using Dirichlet boundary conditions and simple one-step Euler integration. This was the fastest technique available to us at the time of our calculations, though it is now superseded by the reference solution methods of Refs. 4 and 5. The parameters controlling the accuracy of the integration—step size, end points of the integration in the coordinate $\mathbf{R}$, the number of channels included in the expansion Eq. (2), and the accuracy of the numerical integration for the potential matrix elements $V_{mn}(\mathbf{R})$ in Eq. (4)—were chosen such that each individual transition probability was converged to within 1% of its "true" value and detailed balance error, as measured by the quantity

$$e_{mn}=[(P_{mn}-P_{nm})/P_{mn}]\times 100\%, \tag{8}$$

was limited to 0.1%–0.4%, allowing us to report only one probability of each equivalent pair $P_{mn}$, $P_{nm}$.

In the first section of this paper, we define the coordinates for the one-dimensional or collinear atom–diatom and diatom–diatom collisions with vibrational excitation. We then specify numerical values of parameters used to define the three models of the $H_2$–$H_2$ collision. Two of these models are atom–diatom type, one of which takes the potential for the diatom vibration as the harmonic potential, the other as the Morse potential. The third model is the diatom–diatom type, with each diatom being a harmonic vibrator. Masses of the atoms and diatoms are chosen such that all three models are appropriate for the $H_2$–$H_2$ collision—this requires the atom mass to equal the total mass of the diatom. Finally, a Lennard-Jones interaction potential is assumed to operate between the nearest atoms in the collision partners. This is a more realistic choice than the more common one of an exponential potential, at least at low collision energies. In Sec. II we present the numerical results for the transition probabilities. We contrast the physical behavior of the models for qualitative insight into the effects of vibrational anharmonicity and internal structure in the collision partners, and comment briefly on related semiclassical and classical calculations. Finally, we conclude that the simpler exponential interaction potential is preferable to the Lennard-Jones potential because it reproduces transition probabilities for the latter very accurately while requiring far less computing time.

## I. NATURE OF THE THREE MODEL CALCULATIONS

### A. The Atom–Diatom Collision in One Dimension

The original coordinates for this system are simply the positions $x_1$, $x_2$, $x_3$ of the three masses $m_1$, $m_2$, $m_3$, with $m_1-m_2$ comprising the bound or diatomic system. The operator for the Hamiltonian minus the energy eigenvalue is

$$H-E=-\frac{\hbar^2}{2m_1}\frac{\partial^2}{\partial x_1^2}-\frac{\hbar^2}{2m^2}\frac{\partial^2}{\partial x_2^2}-\frac{\hbar^2}{2m_3}\frac{\partial^2}{\partial x_3^2}+V_{12}'(x_2-x_1)+V_I'(x_3-x_2)-E. \tag{9}$$

The interaction potential $V_I'(x_1-x_3)$ has been neglected. We show in the Appendix that several consecutive transformations of coordinates can be performed which (1) put the system into the form of an "atom" colliding with another, oscillating atom bound to an equilibrium position—a two-body problem; see Fig. 1—and (2) reduce all coordinates, masses, and potential parameters to a smaller number of dimensionless quantities. The operator $H-E$ in new units and coordinates is

$$H-E=-1/2\mu(\partial^2/\partial x^2)-\tfrac{1}{2}(\partial^2/\partial y^2)+V_{12}(y)+V_I(x-y)-E, \tag{10}$$

where the energy $E$ is exclusive of center-of-mass mo-

tion and is measured in units of $\hbar\omega$, twice the ground-state vibrational energy of the oscillator $m_1-m_2$. The set of parameters for the collision reduces to $E$, $\mu$, and the parameters of the two potentials.

Next we make the channel expansion, Eq. (2). The function $\phi_n(y)$ representing bound states of the oscillator are solutions of the eigenvalue equation

$$[-\tfrac{1}{2}(\partial^2/\partial y^2)+V_{12}(y)-\epsilon_n]\phi_n(y)=0. \qquad (11)$$

Again, the energies $\epsilon_n$ are measured in units of twice the ground-state oscillator energy, so that for the ground state, $\epsilon_1=\frac{1}{2}$. Two models for the oscillator have been used in our calculations: (1) the harmonic oscillator, for which

$$V_{12}(y)=\tfrac{1}{2}y^2,$$
$$\epsilon_n=n-\tfrac{1}{2}, \qquad n=1, 2, 3, \cdots,$$
$$\phi_n(y)=[2^{n-1}(n-1)!]^{-1/2}H_{n-1}(y)\exp(-y^2/2), \qquad (12)$$

where $H_n$ is the Hermite polynomial, and (2) the Morse oscillator, for which

$$V_{12}(y)=D_e(e^{-2\beta y}-e^{-\beta y}),$$
$$\epsilon_n=[2(2D_e)^{1/2}/\beta](n-\tfrac{1}{2})-\tfrac{1}{2}\beta^2(n-\tfrac{1}{2})^2,$$
$$\phi_n(y)=N_n\exp(-de^{-\beta y})(2de^{-\beta y})^{(k-2n+1)/2}\times L_{k-n}{}^{k-2n+1}(2de^{-\beta y}), \qquad (13)$$

with

$$d=(2D_e)^{1/2}/\beta,$$
$$k=2d,$$
$$N_n=\text{normalization constant}, \qquad (13')$$

and where $L_{a+n}{}^n(x)$ is a generalized Laguerre polynomial. The quantity $D_e$ is the depth of the potential well, and $\beta$ is an anharmonicity parameter. The Morse oscillator has a finite number of bound states, up to $n_{\max}=k$. The CC equations for both models have the form

$$(d^2/dx^2+k_n^2)f_n(x)=2\mu\sum_{m=1}^{n_{tot}}V_{nm}(x)f_m(x), \qquad (14)$$

with

$$k_n^2=2\mu(E-\epsilon_n),$$
$$V_{nm}(x)=\langle\phi_n(y)\mid V_I(x-y)\mid\phi_m(y)\rangle=\int_{-\infty}^{\infty}dy\phi_n(y)V_I(x-y)\phi_m(y),$$
$$n_{tot}=\text{number of states retained in the channel expansion.} \qquad (14')$$

Our choice of the interaction potential $V_I(x-y)$ is the Lennard-Jones potential with its singularity at $x-y=0$ replaced by a finite step.

$$V_I(x-y)=4\epsilon\{[\sigma/(x-y)]^{12}-[\sigma/(x-y)]^6\}, \quad x-y\geq b$$
$$=V_I(b), \quad x-y<b, \qquad (15)$$

although another choice, the exponential potential,

$$V_I(x-y)=C\exp[-\alpha(x-y)] \qquad (16)$$

was used to check our method by duplicating some calculations of Secrest and Johnson.[3]

As a shorthand notation for the two models let us use HOLJ for the harmonic oscillator hit by an atom interacting with it by a Lennard-Jones potential, and MOLJ for the Morse oscillator and the same Lennard-Jones interaction (and HOEXP for the harmonic oscillator and the exponential potential). In all of these calculations, the parameters $\mu$, $\epsilon$, $\sigma$ (and also $D_e$, $\beta$ for the MOLJ case) were chosen to represent the collision of two hydrogen molecules, one of which has its vibrational degree of freedom frozen out. The dimensionless values of the parameters are then

$$\mu=0.5,$$
$$\epsilon=5.707\times10^{-3},$$
$$\sigma=46.71,$$
$$D_e=8.3255,$$
$$\beta=0.24886, \qquad (17)$$

as converted from dimensioned quantities quoted in Bhatia[6a] and Herzberg[6b] and Herzfeld and Litovitz.[6c] A slight adjustment of $\beta$ from a calculated value of 0.24840 was made to obtain the proper value of $\epsilon_1=0.5$ for the ground vibrational level. The values of $D_e$ and $\beta$ allow 16 bound levels for the Morse oscillator.

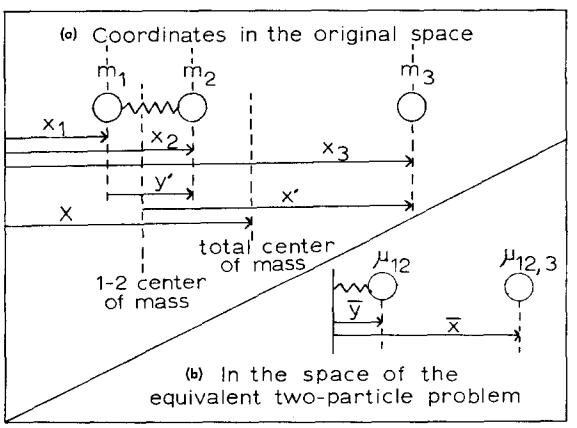


FIG. 1. The original (a) and transformed (b) coordinates for the atom–diatom collision in one dimension.

### B. The Diatom–Diatom Collision in One Dimension

The original coordinates for this system are the positions $x_i$ ($i=1, 2, 3, 4$) of the four masses $m_i$, with $m_1-m_2$ and $m_3-m_4$ forming the two bound diatomic systems. Assuming the dominant nonbound interaction

TABLE I. Selection of channels to include in diatom–diatom problem. Maximum excitation of each diatom is to second vibrational level $n_i=2$.[a]

| Method (1)—form all possible product states $(n_1, n_2)$ with $n_1$, $n_2$ independently ranging from 1 to 4 | | | | Method (2)—add the restriction $n_1+n_2\leq 4$ | |
|---|---|---|---|---|---|
| Channel no.[b] | $(n_1, n_2)$ | Channel no. | $(n_1, n_2)$ | Channel no.[b] | $(n_1, n_2)$ |
| **1** | **1, 1** | 9 | 3, 1 | **1** | **1, 1** |
| **2** | **1, 2** | 10 | 3, 2 | **2** | **1, 2** |
| 3 | 1, 3 | 11 | 3, 3 | **3** | **2, 1** |
| 4 | 1, 4 | 12 | 3, 4 | 4 | 1, 3 |
| **5** | **2, 1** | 13 | 4, 1 | 5 | 2, 2 |
| 6 | 2, 2 | 14 | 4, 2 | 6 | 3, 1 |
| 7 | 2, 3 | 15 | 4, 3 | 7 | 1, 4 |
| 8 | 2, 4 | 16 | 4, 4 | 8 | 2, 3 |
| | | | | 9 | 3, 2 |
| | | | | 10 | 4, 1 |

[a] Values of $n_i$ to 4 should be included on the basis of atom–diatom model results.

[b] In each selection scheme the open channels are in bold face.

$V_I$ to be between particles 2 and 3, one has

$$H-E=\sum_{i=1}^{4}-(\hbar^2/2m_i)(\partial^2/\partial x_i^2)+V_{12}'(x_1-x_2)+V_{34}'(x_3-x_4)+V_I'(x_2-x_3)-E. \quad (18)$$

In the Appendix we show that successive coordinate transformations, analogous to those used to reduce the atom–diatom problem, put the system into the form of a diatom oscillator hitting a bound oscillating "atom." The system parameters are also made dimensionless. The operator $H-E$ in the transformed coordinates is

$$H-E=-(1/2\mu)(\partial^2/\partial x^2)-\tfrac{1}{2}(\partial^2/\partial y_1^2)-\tfrac{1}{2}(\partial^2/\partial y_2^2)+V_{12}(y_1)+V_{34}(y_2)+V_I(x-y_1-y_2)-E \quad (19)$$

for a system of two *identical* diatoms; the general form is given in the Appendix. Again, $E$ is the energy, exclusive of center-of-mass motion, in units of twice the ground vibrational energy of either oscillator. The set of parameters remains $E$, $\mu$, and the parameters of the potentials, as in Sec. I.A. The diatom–diatom collision can be made physically equivalent to the atom–diatom collision, so that comparisons of analogous transition probabilities will illustrate the effect of an internal degree of freedom in the incident "particle." In addition, "resonant" energy transfer involving interchange of vibrational quanta between the diatoms with no conversion of translational energy exists for the diatom–diatom case.

The channel expansion of Eq. (2) takes the form

$$\psi(x, y_1, y_2)=\sum_n f_n(x)\phi_{n1}(y_1)\phi_{n2}(y_2), \quad (20)$$

where the $\phi_{n1}$, $\phi_{n2}$ are solutions of eigenvalue equations of the form (10). In our calculations, both diatom oscillators are modeled as harmonic oscillators and the interaction potential is the Lennard-Jones potential; this model is denoted by the shorthand HOHOLJ. System parameters exclusive of the energy $E$ are

$$\mu=0.5,$$
$$\epsilon=5.707\times10^{-3},$$
$$\sigma=46.71. \quad (21)$$

Test calculations on a model with the exponential potential successfully duplicated the results of Riley.[1]

The CC equations have the general form

$$(\partial^2/\partial x^2+k_n^2)f_n(x)=2\mu\sum_m V_{nm}(x)f_m(x), \quad (22)$$

where

$$k_n^2=2\mu(E-\epsilon_{n1}-\epsilon_{n2}),$$

$$V_{nm}(x)=\langle\phi_{n1}(y_1)\phi_{n2}(y_2)\mid V_I(x-y_1-y_2\mid\phi_{m1}(y_1)\phi_{m2}(y_2)\rangle.$$

The ordering of states in the expansion (20) becomes significant when we truncate the expansion. Two ways to order or include channels suggest themselves: (1) retain a certain number of states for each oscillator, yielding the correspondence between $n$ and $(n1, n2)$ given in the left-hand columns of Table I, or (2) retain product states $(n1, n2)$ up to a certain energy level $\epsilon_{n1}+\epsilon_{n2}$, yielding the correspondence of $n$ and $(n1, n2)$ given in the right-hand columns of Table I. The second approach places all open channels together at the beginning of the numbering scheme, and makes for a smaller set of coupled equations for similar accuracy; that is, the states $(n1, n2)$ where both $n1$ and $n2$ are high virtual states will be relatively unimportant. The second approach will be used in our HOHOLJ calculations.

Note the occurrence of equivalent channels $(n1, n2)\leftrightarrow(n2, n1)$. These channels are physically distinct; a transition from one to the other involves no conversion of translational into vibrational energy—it is a *resonant* energy transfer.

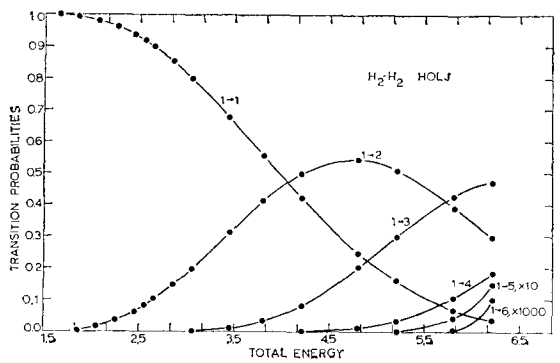


FIG. 2. Energy dependence of the transition probabilities $P(1\rightarrow n)$ from the ground state in the atom–diatom problem, HOLJ model.

TABLE II. Calculated transition probabilities for HOLJ model. Numbers in parentheses are negative powers of 10 multiplying result.[a]

| | $E$[b] | | | | | |
|---|---|---|---|---|---|---|
| $P_{n\to m}$ | 1.55 | 1.65 | 1.85 | 2.05 | 2.25 | |
| 1→1 | 0.9999 | 0.9992 | 0.9946 | 0.9835 | 0.964 | |
| 1→2 | 0.121(3) | 0.792(3) | 0.538(2) | 0.165(1) | 0.357(1) | |
| 2→2 | 0.9999 | 0.9992 | 0.9946 | 0.9835 | 0.964 | |
| | $E$ | | | | | |
| $P_{n\to m}$ | 2.45 | 2.55 | 2.65 | 2.85 | 3.05 | 3.45 |
| 1→1 | 0.936 | 0.918 | 0.898 | 0.852 | 0.799 | 0.674 |
| 1→2 | 0.638(1) | 0.815(1) | 0.101 | 0.147 | 0.199 | 0.314 |
| 1→3 | | 0.506(5) | 0.411(4) | 0.406(3) | 0.170(2) | 0.109(1) |
| 2→2 | 0.936 | 0.918 | 0.897 | 0.843 | 0.771 | 0.580 |
| 2→3 | | 0.235(3) | 0.152(2) | 0.100(1) | 0.296(1) | 0.105 |
| 3→3 | | 0.99976 | 0.9984 | 0.990 | 0.969 | 0.884 |
| | $E$ | | | | | |
| $P_{n\to m}$ | 3.80 | 4.20 | 4.80 | 5.20 | 5.80 | 6.20 |
| 1→1 | 0.555 | 0.420 | 0.245 | 0.157 | 0.687(1) | 0.351(1) |
| 1→2 | 0.412 | 0.498 | 0.543 | 0.510 | 0.394 | 0.296 |
| 1→3 | 0.323(1) | 0.799(1) | 0.201 | 0.300 | 0.427 | 0.470 |
| 1→4 | 0.421(4) | 0.855(3) | 0.106(1) | 0.322(1) | 0.105 | 0.183 |
| 1→5 | | | 0.107(4) | 0.264(3) | 0.422(2) | 0.149(1) |
| 1→6 | | | | | 0.350(5) | 0.100(3) |
| 2→2 | 0.384 | 0.179 | 0.104(1) | 0.222(1) | 0.175 | 0.299 |
| 2→3 | 0.202 | 0.313 | 0.383 | 0.328 | 0.148 | 0.416(1) |
| 2→4 | 0.640(3) | 0.870(2) | 0.631(1) | 0.136 | 0.258 | 0.297 |
| 2→5 | | | 0.123(3) | 0.228(2) | 0.241(1) | 0.644(1) |
| 2→6 | | | | | 0.341(4) | 0.773(3) |
| 3→3 | 0.755 | 0.536 | 0.177 | 0.313(1) | 0.387(1) | 0.134 |
| 3→4 | 0.982(2) | 0.698(1) | 0.238 | 0.326 | 0.297 | 0.180 |
| 3→5 | | | 0.108(2) | 0.137(1) | 0.878(1) | 0.170 |
| 3→6 | | | | | 0.233(3) | 0.401(2) |
| 4→4 | 0.989 | 0.921 | 0.676 | 0.421 | 0.805(1) | 0.364(2) |
| 4→5 | | | 0.124(1) | 0.834(1) | 0.256 | 0.317 |
| 4→6 | | | | | 0.156(2) | 0.186(1) |
| 5→5 | | | 0.986 | 0.900 | 0.612 | 0.338 |
| 5→6 | | | | | 0.146(1) | 0.945(1) |
| 6→6 | | | | | 0.9835 | 0.882 |

[a] Calculated values of $P_{nm}$ and $P_{mn}$ were always well within 1% of each other. To avoid redundancy, only the former are given.

[b] Energy units are $\hbar\omega$, twice the ground-state vibrational energy of the diatom.

## II. RESULTS OF MODEL CALCULATIONS

Tables II–IV present our calculated transition probabilities for the HOLJ, MOLJ, and HOHOLJ models. The total error in these results is in the range of 1% or less. The behavior of selected probabilities $P_{mn}$ as functions of energy is illustrated in Figs. 2–6. The clearest feature for both atom–diatom models HOLJ and MOLJ, which cover significant energy ranges, is the oscillation of the $P_{mn}$. For instance, the elastic transition probability $P_{22}$ in the HOLJ model decreases steadily until it reaches a deep minimum near $E=4.9$; then, despite the opening of an additional *in*elastic channel at $E=4.5$, $P_{22}$ begins to rise rapidly. This is "caused" by the

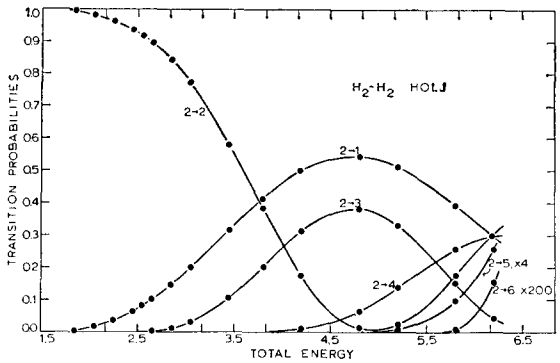


FIG. 3. Energy dependence of the transition probabilities $P(2\rightarrow n)$ from the first excited state in the atom–diatom problem, HOLJ model.

downward turns in probabilities $P_{21}$ and $P_{23}$. We see a similar behavior in transitions from initial states 1 and 3, $P_{1n}$ and $P_{3n}$. Comparing transitions according to their initial state, we note that the coupled oscillations in probabilities set in at a lower value of initial kinetic energy $E-\epsilon_n$, the higher the initial state $n$.

This oscillatory behavior has been found in similar atom–diatom model systems by previous workers. Shuler and Zwanzig[7] found sharp-peaked oscillations for all transitions in their exact but specialized quantum-mechanical treatment of the harmonic diatom and the hard-sphere interaction potential,

$$V_I(x-y)=0, \quad x-y>0.$$
$$\infty, \quad x-y=0. \qquad (23)$$

The exact result of Secrest and Johnson[3] for several HOEXP models show maxima in inelastic probabilities. The exact semiclassical results of Rapp and Sharp[8] for a HOEXP-like model show regular oscillations. The oscillations in our results and the results quoted above are real, although there have been many approximate calculations in which the use of low-order perturbation theory or the artificial exclusion of most of the channels in expansion (2) has led to a spurious effect.

A major part of the analysis of our results is the

TABLE III. Calculated transition probabilities for MOLJ model.[a]

| | $E$[b] | | | |
|---|---|---|---|---|
| $P_{n\rightarrow m}$ | 1.55 | 1.90 | 2.30 | 2.75 |
| 1→1 | 0.99983 | 0.9958 | 0.980 | 0.939 |
| 1→2 | 0.165(3) | 0.417(2) | 0.198(1) | 0.604(1) |
| 1→3 | | | | 0.129(3) |
| 2→2 | 0.99983 | 0.9958 | 0.980 | 0.931 |
| 2→3 | | | | 0.819(2) |
| 3→3 | | | | 0.9917 |
| | $E$ | | | |
| $P_{n\rightarrow m}$ | 3.40 | 4.15 | 4.45 | 4.85 |
| 1→1 | 0.854 | 0.724 | 0.662 | 0.582 |
| 1→2 | 0.142 | 0.255 | 0.302 | 0.354 |
| 1→3 | 0.314(2) | 0.204(1) | 0.345(1) | 0.602(1) |
| 1→4 | 0.159(5) | 0.306(3) | 0.977(3) | 0.320(2) |
| 1→5 | | 0.138(6) | 0.317(5) | 0.394(4) |
| 1→6 | | | | 0.198(7) |
| 2→2 | 0.780 | 0.508 | 0.391 | 0.249 |
| 2→3 | 0.779(1) | 0.229 | 0.287 | 0.347 |
| 2→4 | 0.868(4) | 0.809(2) | 0.198(1) | 0.475(1) |
| 2→5 | | 0.623(5) | 0.111(3) | 0.104(2) |
| 2→6 | | | | 0.764(6) |
| 3→3 | 0.915 | 0.643 | 0.493 | 0.296 |
| 3→4 | 0.412(2) | 0.108 | 0.182 | 0.281 |
| 3→5 | | 0.182(3) | 0.230(2) | 0.145(1) |
| 3→6 | | | | 0.180(4) |
| 4→4 | 0.9958 | 0.878 | 0.756 | 0.531 |
| 4→5 | | 0.598(2) | 0.407(1) | 0.137 |
| 4→6 | | | | 0.371(3) |
| 5→5 | | 0.9938 | 0.957 | 0.838 |
| 5→6 | | | | 0.919(2) |
| 6→6 | | | | 0.9904 |

[a] Calculated values of $P_{nm}$ and $P_{mn}$ were always well within 1% of each other. To avoid redundancy, only the former are given.

[b] Energy units are $\hbar\omega$, twice the ground-state vibrational energy of the diatom.

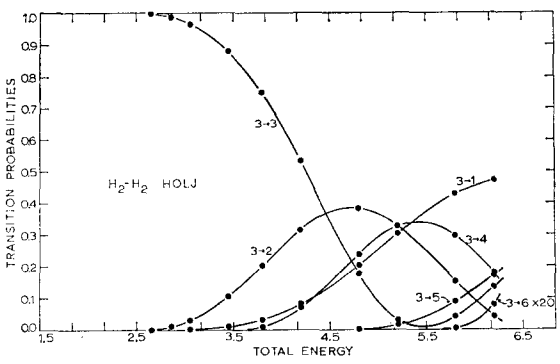


FIG. 4. Energy dependence of the transition probabilities $P(3\rightarrow n)$ from the second excited state in the atom–diatom problem, HOLJ model.

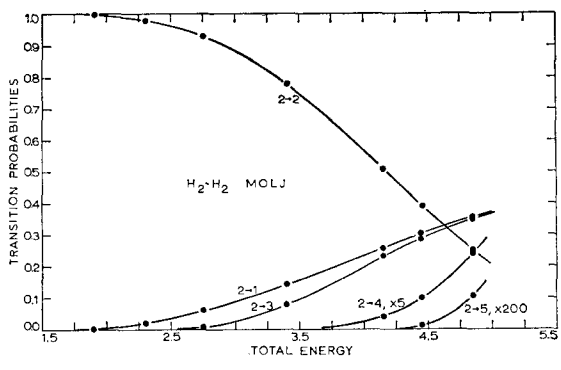


FIG. 5. Energy dependence of the transition probabilities $P(2\rightarrow n)$ from the first excited state in the atom–diatom problem, MOLJ model.

TABLE IV. Calculated transition probabilities for HOHOLJ model.[a]

| | $E$[b] | | | | | |
|---|---|---|---|---|---|---|
| $P_{n\to m}$ | 2.05 | 2.15 | 2.35 | 2.55 | 2.75 | 2.95 |
| 11→11[c] | 0.99990 | 0.99934 | 0.9956 | 0.987 | 0.972 | 0.951 |
| 11→12 | 0.508(4) | 0.329(3) | 0.219(2) | 0.656(2) | 0.140(1) | 0.245(1) |
| 12→12 | 0.9929 | 0.980 | 0.950 | 0.914 | 0.872 | 0.825 |
| 12→21 | 0.707(2) | 0.194(1) | 0.474(1) | 0.789(1) | 0.114 | 0.150 |

| | $E$ | | | |
|---|---|---|---|---|
| $P_{n\to m}$ | 3.08 | 3.15 | 3.35 | 3.55 |
| 11→11 | 0.934 | 0.923 | 0.890 | 0.853 |
| 11→12 | 0.328(1) | 0.382(1) | 0.547(1) | 0.731(1) |
| 11→13 | 0.183(5) | 0.680(5) | 0.648(4) | 0.261(3) |
| 11→22 | 0.366(5) | 0.136(4) | 0.130(3) | 0.523(3) |
| 12→12 | 0.792 | 0.773 | 0.714 | 0.650 |
| 12→21 | 0.175 | 0.188 | 0.224 | 0.258 |
| 12→13 | 0.192(3) | 0.603(3) | 0.381(2) | 0.108(1) |
| 12→22 | 0.104(3) | 0.329(3) | 0.214(2) | 0.627(2) |
| 12→31 | 0.143(4) | 0.548(4) | 0.524(3) | 0.204(2) |
| 13→13 | 0.980 | 0.963 | 0.909 | 0.846 |
| 13→22 | 0.200(1) | 0.360(1) | 0.848(1) | 0.136 |
| 13→31 | 0.110(3) | 0.352(3) | 0.203(2) | 0.556(2) |
| 22→22 | 0.960 | 0.927 | 0.826 | 0.715 |

[a] Calculated values of $P(n1, n2)\to(n1', n2')$ that should be equal among themselves by time-reversal invariance or symmetry were negligibly different. Only one member is given to avoid redundancy.

[b] Energy units are $\hbar\omega_{12}=\hbar\omega_{34}=\hbar\omega$, twice the ground-state vibrational energy of either diatom.

[c] The transition $(n1, n2)\to(n1', n2')$ is abbreviated to $n1n2\to n1'n2'$.

comparison and contrast of the three models for the $H_2$–$H_2$ collision. Suitable quantities for comparison include analogous transition probabilities (as 1→2 HOLJ, 1→2 MOLJ, 11→12⊕11→21 HOHOLJ), net energy transfer from analogous initial states, and relative strengths of multiquantum jumps. Contrasts of HOLJ and MOLJ models will tell us something about the effects of anharmonicity, and contrasts of HOLJ and HOHOLJ will help reveal the effect of internal structure in the incident particle. At the same time, examinations of models individually show the basic energy behavior of the probabilities and other properties that are as instructive as the obvious contrasts between models. Specific items we can study, both within and between models, include comparisons of (1) all transi-

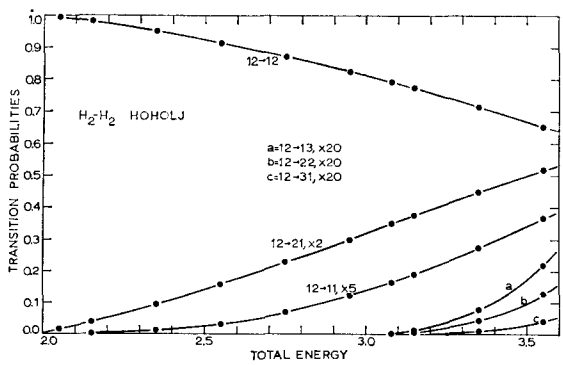


FIG. 6. Energy dependence of the transition probabilities $P(12\to mn)$ in the diatom-diatom problem, HOHOLJ model. The initial state 1–2 has one of the diatoms in its ground state, the other in its first excited state.

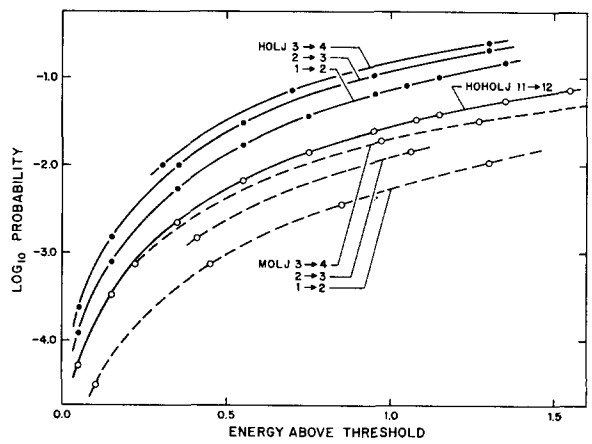


FIG. 7. Demonstration of very similar energy dependence for one-quantum jumps in all three models of the $H_2$–$H_2$ collision, HOLJ, MOLJ, HOHOLJ. The curves of $\log_{10}$(probability) have been biased by −0.75 in the MOLJ cases for clarity.

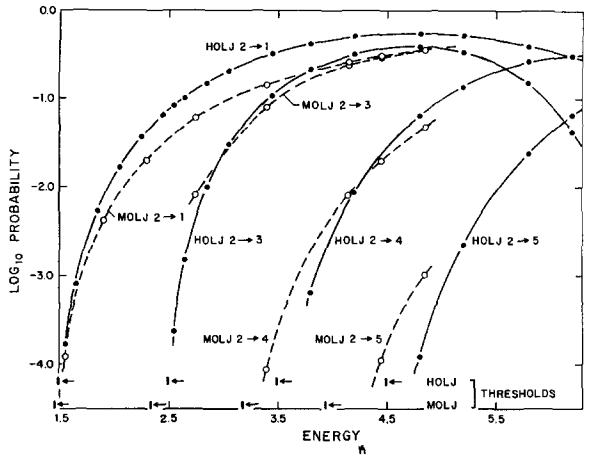


FIG. 8. Comparison of all transition probabilities $P(2\rightarrow n)$ from the first excited state. The two atom–diatom models HOLJ and MOLJ are both represented.

tions of a given type, such as one-quantum jumps $P_{n,n+1}$, for various initial states $n$, (2) all transitions $P_{nm}$ from a given initial state $n$, (3) net energy transfer (translational to vibrational) from each state $n$, defined for the atom–diatom models as

$$\langle \Delta E_n \rangle = \sum_m{}' P_{nm}(\epsilon_m - \epsilon_n), \qquad (24)$$

where the $\epsilon_i$ are the energy eigenvalues for the diatom vibration. The diatom–diatom model has several types of energy transfer that will be defined later.

Figure 7 presents a logarithmic plot of several one-quantum jump probabilities for each of the three models. The abscissa in each case is energy above threshold $E_{ex}=E-\epsilon_{n+1}$, rather than initial kinetic energy. The striking fact brought out by the logarithmic plot is that all the $P_{n,n+1}$ for a given model behave much like

$$P_{n,n+1}(E) = \mathrm{Const}_n f(E_{ex}), \qquad (25)$$

with $f(_{ex})$ the same for all $n$. Further, $f(E)$ is very similar for the HOLJ and HOHOLJ models, while $\log f(E)$ for MOLJ has a smaller slope at the lowest energies. Pursuing this point of similarity, we turn to the actual magnitudes of probabilities at low energy. For the analogous transitions $11\rightarrow 12 \oplus 11\rightarrow 21$ HOHOLJ and $1\rightarrow 2$ HOLJ, we find

$$(P_{11\rightarrow 12}+P_{11\rightarrow 21})_{\mathrm{HOHOLJ}}/(P_{12})_{\mathrm{HOLJ}} \approx 0.8 \qquad (26)$$

at low energy. Not only do these transitions have similar $f(E)$ or "slopes," but their magnitudes are close, being reduced for the HOHOLJ case by the extra adiabaticity or softness introduced into the collision process by the extra internal degree of freedom. That the change from HOLJ to HOHOLJ is principally the addition of a very modest amount of adiabaticity is supported by comparing the $11\rightarrow 12$ and $21\rightarrow 22$ HOHOLJ probabilities. The two values are extremely close at low energies, indicating again that the initial state of our extra internal degree of freedom has little effect of itself on transition probabilities—which would not be true if the extra degree of freedom coupled strongly to translation. However, it does couple strongly to the vibration of the other diatom, giving rise to highly favored resonant energy transfers of the type $12\rightarrow 21$. The latter transitions may be of independent interest, but they do not drain much probability from other transitions at modest energies.

Proceeding to the HOLJ–MOLJ comparison, we find the ratio $(P_{12})_{\mathrm{MOLJ}}/(P_{12})_{\mathrm{HOLJ}}$ is quite small—around 0.3–0.4. This is readily explained by the lower coupling between adjacent states of the anharmonic oscillator (compared to that for a harmonic oscillator) induced by a potential that is essentially linear in the oscillator coordinate. This near linearity in the coordinate $y$ holds near the classical turning point $x_t$, where $V_I(x_t-\langle y\rangle)=E-\epsilon_n$, for our Lennard-Jones potential—and it is the region of $x_t$ that is most important. The problem of why MOLJ one-quantum jumps have a different "slope" at low energies than HOLJ jumps cannot be commented on with our calculations limited to so few energies.

Figure 8 presents a comparison of the second type, among all transitions from initial state 2 ($P_{21}$, $P_{23}$, $P_{24}$, $P_{25}$) for both atom–diatom models. It is also a logarithmic plot, and the abcissa is appropriately the total energy $E$. A clear feature is that the horizontal or energy gaps between adjacent curves $2\rightarrow n$, $2\rightarrow n+1$ are widening as $n$ increases. That is, in either of the two models, the higher the quantum jump, the more slowly the probability grows. The explanation is again in the essential linearity of the interaction potential at the classical turning point; the first-order coupling of a final state to the initial state is a very strongly decreasing function of the number of quantum jumps in the transition. This argument does not hold as well for the anharmonic MOLJ model, and so the energy intervals between the various curves do not widen as

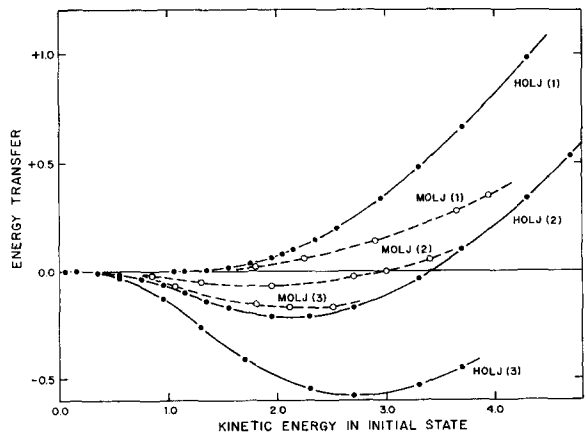


FIG. 9. Atom–diatom collision: net transfer of energy from translation to diatom vibration, as a function of the initial state ($n$) and of the kinetic energy in the initial state. Both HOLJ and MOLJ models are represented.

rapidly here, even after we discount the decreasing intervals between thresholds.

We have no HOHOLJ results for transitions higher than two-quantum jumps, and these only from the ground state. Yet the HOHOLJ model has a greater variety of transition types or processes than the atom–diatom models. Finding the relative magnitudes of the different processes is a worthwhile task. The processes we distinguish, and examples of each, are:

E—Elastic: 11→11, 12→12

R—Resonant: no net quantum jump in the pair of diatoms, i.e., opposite jumps in each diatom: 12→21, 22→13

SR—Semiresonant: opposite jumps of different order in each diatom: 12→31

NR—Nonresonant:

(a) One-quantum jump: 11→12, 22→12

(b) Two-quantum jump: 11→13

(c) Double one-quantum jump: 11→22

The HOHOLJ results at the modest energy $E=3.55$ show that the strengths of processes generally follow the order

$$\mathrm{E}>\mathrm{R}>\mathrm{NR(a)}>\mathrm{SR}>\cdots, \qquad (27)$$

reflecting the weakness of translational–vibrational coupling compared to vibrational–vibrational (V–V) coupling. There are V–V processes that are weak, as the 13→31 transition involving concerted two-quantum jumps that are approximately forbidden in first order.

Our final study is of energy transfer. Figure 9 plots $\langle \Delta E_n \rangle$ for both atom–diatom models from initial states 1, 2, and 3 as functions of initial kinetic energy. MOLJ has about 40% the energy transfer efficiency of HOLJ, from the initial states 1 or 2. The energy transfer in state 2 reaches a node at lower energy for MOLJ than HOLJ, reflecting the earlier opening up of new channels for MOLJ. The disparity in form for HOLJ and MOLJ energy transfer appears to be very pronounced for high initial states.

To define the measure of energy transfer for diatom–diatom collisions, we must denote the subsystems or degrees of freedom between which the transfer occurs. These subsystems are translation or "tr," diatom 1–2 or "d" (playing the same role as the diatom in atom–diatom collisions), and diatom 3–4 or "a" (playing the same role as the atom). The energy transfers most directly comparable to the atom–diatom results are tr→a+d≡tr→all, tr→d (not equal in general to tr→a; "d" and "a" may be initially in different states, making for distinguishability in this otherwise symmetric system), and tr+a→d≡all→d. Figure 10 presents these three $\langle \Delta E \rangle$ functions for HOHOLJ in initial states 11, 12, and 13, plotted as functions of initial kinetic energy. $\Delta E$(tr→d) is very nearly identical for states 11 and 12 for comparable distances above their respective thresholds, corresponding to our finding that the state of a does not much affect the coupling of d to tr. There is

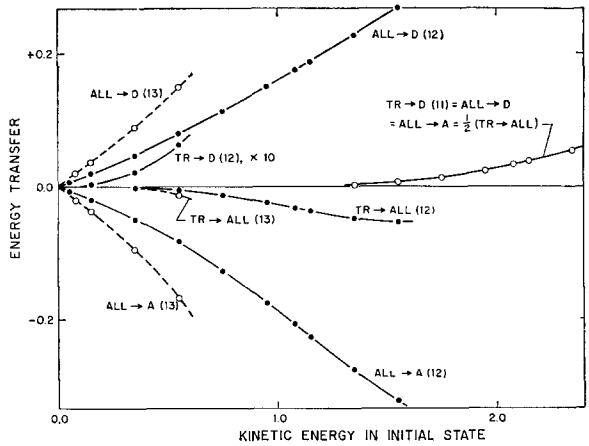


FIG. 10. Diatom–diatom collision, HOHOLJ model: net transfer of energy between the various degrees of freedom (e.g., TR = translation; see text for symbol meaning), as a function of initial state $(n_1 n_2)$ and of the kinetic energy in the initial state.

also the expected trend, that $\Delta E$(all→d) increases strongly as the state of "a" is raised. As there is nothing surprising within Fig. 10, we proceed to compare HOHOLJ with HOLJ via their ratio $\Delta E(\mathrm{tr}\rightarrow\mathrm{all})/\Delta E$ for analogous initial states. For HOHOLJ state 11 and HOLJ state 1, the ratio is around 0.8, reflecting the extra adiabaticity of the diatom–diatom case. For HOHOLJ state 21 and HOLJ state 2, the ratio is about 0.4, probably due to the drain of the resonant process 12→21. The same ratio occurs in the comparison HOHOLJ 31↔HOLJ 3 and in the weaker comparison HOHOLJ 22↔HOLJ 3.

We may draw a number of conclusions from our results, particularly regarding the value of similar model calculations on intermolecular energy transfer. Despite the limitations of our models—one-dimensionality, a restricted and modeled interaction potential, and the simplicity of the models of the diatoms—we have extracted a number of physical insights into the collision of two fairly stiff diatoms, if not into the actual $H_2$–$H_2$ collision. The effects of anharmonicity and of internal degrees of freedom, and the relative magnitudes of different processes are among the insights. Certainly, calculations on a wider sampling of collision partners within the same general modeling scheme can be recommended as a practical and valuable project; the computing times are moderate. We are also able to suggest some precautions and some simplifications in modeling a collision system. First, the introduction of all the internal degrees of freedom of the collision partners is not as necessary for reasonably accurate calculations as a fair degree of anharmonicity in the vibrations. Neither complication can really be ignored and semiempirical corrections based on careful studies of additional systems are probably desirable. Secondly, the choice of analytic form for the interaction potential is not nearly as important as the careful estimation of the parameters for the chosen form. To support this claim

we turn to some results of A. Wagner of this laboratory. In entirely similar calculations he employed HOEXP and HOHOEXP models for the $H_2$–$H_2$ system with the EXP (exponential) potential parameter $\alpha$ carefully fitted by various least-squares techniques to the Lennard-Jones parameters $\sigma$, $\epsilon$. His calculations duplicated ours within several percent for all but the highest quantum jumps at the highest energies, where one probability might be off as much as a factor of 2. Let us consider that neither LJ nor EXP potentials are terribly realistic, and that the change in probabilities in switching from one to the other is less than the change produced by a very minor shift in the parameters of either one. We see no reason to retain the LJ potential with its attendant great increase in complexity and computing time,[9] at least in treating systems such as ours where the energy quanta exchanged in collision are considerably larger than the small attractive well in the LJ potential. If one *must* use a potential that has an appreciable attractive portion, as a chemical "well," or if one must do accurate calculations, his best choice of potential is one tabulated numerically. If one is satisfied with as simple a potential as the exponential, he should choose his parameters very carefully. A much-needed study is the development of simple but more adequate model intermolecular potentials, particularly for three-dimensional systems.

## ACKNOWLEDGMENTS

One of us (D. D.) wishes to thank the California Institute of Technology for its hospitality. We would like to thank A. Wagner, N. W. Winter, and D. G. Truhlar of the California Institute of Technology for helpful discussions. We are particularly grateful to Merle E. Riley, presently at the Harvard College Observatory, for a thorough and helpful criticism of the manuscript and for other suggestions.

## APPENDIX

### Transformation to Dimensionless Coordinates for the Atom–Diatom Problem

Figure 1(a) shows the original coordinate system. The first step is to separate the center of mass motion in Eq. (9), by defining new coordinates

$$X=(m_1x_1+m_2x_2+m_3x_3)/M, \qquad M=m_1+m_2+m_3$$

$$=\text{coordinate of center of mass of entire system.}$$

$$x'=x_3-(m_1x_1+m_2x_2)/m, \qquad m=m_1+m_2$$

$$=\text{distance between particle 3 and center of mass of system 1–2,}$$

$$y'=x_2-x_1, \tag{A1}$$

and corresponding masses

$$M\rightarrow X,$$

$$\mu_{12,3}=mm_3/M\rightarrow x'$$

$$\mu_{12}=m_1m_2/m\rightarrow y'. \tag{A2}$$

The new form of the operator $H-E$ is

$$-\frac{\hbar^2}{2M}\frac{\partial^2}{\partial X^2}-\frac{\hbar^2}{2\mu_{12,3}}\frac{\partial^2}{\partial x'^2}-\frac{\hbar^2}{2\mu_{12}}\frac{\partial^2}{\partial y'^2}$$
$$+V_{12}(y')+V_I[x'-(m_1/m)y']-E. \tag{A3}$$

Now remove the center-of-mass motion; write

$$E=E_{\rm tr}+E_{\rm vib}$$
$$=E_{\rm tr}^{\rm cm}+E_{\rm tr}^{\rm rel}+E_{\rm vib}, \tag{A4}$$

and remove the operator

$$-(\hbar^2/2m)(\partial^2/\partial X^2)-E_{\rm tr}^{\rm cm}=0 \quad \text{(for eigenstates)}. \tag{A5}$$

Next, place $x'$ and $y'$ on an equal footing by defining

$$x'=(m_1/m)(\bar{x}+y_0'), \quad \text{or} \quad \bar{x}=(m/m_1)x'-y_0',$$
$$y'=\bar{y}+y_0', \quad \text{or} \quad \bar{y}=y'-y_0', \tag{A6}$$

where $y_0'$ is the equilibrium value of $y'$. The corresponding masses are

$$\bar{\mu}=(m_1^2/m^2)\mu_{12,3}=m_1^2m_3/mM\rightarrow\bar{x},$$
$$\mu_{12}\rightarrow\bar{y}, \tag{A7}$$

and the operator $H-E$ becomes

$$-\frac{\hbar^2}{2\bar{\mu}}\frac{\partial^2}{\partial\bar{x}^2}-\frac{\hbar^2}{2\mu_{12}}\frac{\partial^2}{\partial\bar{y}^2}+\bar{V}_{12}(\bar{y})+\bar{V}_I(\bar{x}-\bar{y})-\bar{E}, \tag{A8}$$

where

$$\bar{V}_{12}(\bar{y})=V_{12}(\bar{y}+\bar{y}_0'),$$
$$\bar{V}_I(\bar{x}-\bar{y})=V_I[(m_1/m)(\bar{x}-\bar{y})],$$
$$\bar{E}=E-E_{\rm tr}^{\rm cm}. \tag{A9}$$

Lastly, divide the whole of Eq. (A8) by $\hbar\omega$ = twice the ground-state vibrational energy of the 1–2 system, and absorb the factors $\hbar^2/2\mu_i$ into the derivative terms. Define

$$x=(\mu_{12}\omega/\hbar)^{1/2}\bar{x},$$
$$y=(\mu_{12}\omega/\hbar)^{1/2}\bar{y},$$
$$\mu=\bar{\mu}/\mu_{12}=m_1m_3/Mm_2,$$
$$E_r=\bar{E}/\hbar\omega \tag{A10}$$

to obtain Eq. (10)

$$-(1/2\mu)(\partial^2/\partial x^2)-\tfrac{1}{2}(\partial^2/\partial y^2)+V_{12}'(y)+V_I'(x-y)-E_r,$$

where

$$V_{12}'(y)=\frac{\bar{V}_{12}[(\hbar/\mu_{12}\omega)^{1/2}y]}{\hbar\omega}$$
$$=\frac{V_{12}[(\hbar/\mu_{12}\omega)^{1/2}y+y_0']}{\hbar\omega},$$
$$V_I'(x-y)=\frac{\bar{V}_I[(\hbar/\mu_{12}\omega)^{1/2}(x-y)]}{\hbar\omega}$$
$$=\frac{V_I[(m/m_1)(\hbar/\mu_{12}\omega)^{1/2}(x-y)]}{\hbar\omega}. \quad \text{(A11)}$$

The transformations in (A11) will change all parameters of the original potentials into dimensionless quantities, and in some cases reduce the number of parameters in $V_{12}$ by one.

### Transformation to Dimensionless Coordinates for the Diatom–Diatom Problem

We separate the center-of-mass motion from Eq. (18) by defining the coordinates and corresponding masses

$$X=\sum^4 m_ix_i/M, \qquad M=m_1+m_2+m_3+m_4,$$
$$y_{12}'=x_2-x_1, \qquad \mu_{12}=m_1m_2/m_{12} \qquad (m_{ij}=m_i+m_j),$$
$$y_{34}'=x_4-x_3, \qquad \mu_{34}=m_3m_4/m_{34},$$
$$x'=(m_3x_3+m_4x_4)/m_{34}-(m_1x_1+m_2x_2)/m_{12},$$
$$\mu_{12,34}=m_{12}m_{34}/M$$
$$=\text{distance between the centers of mass of systems 1–2 and 3–4.} \quad \text{(A12)}$$

The operator $H-E$, dropping the operator (A5), is

$$-\frac{\hbar^2}{2\mu_{12}}\frac{\partial^2}{\partial y_{12}'^2}-\frac{\hbar^2}{2\mu_{34}}\frac{\partial^2}{\partial y_{34}'^2}-\frac{\hbar^2}{2\mu_{12,34}}\frac{\partial^2}{\partial x'^2}+V_{12}(y_{12}')$$
$$+V_{34}(y_{34}')+V_I\left(x'-\frac{m_1}{m_{12}}y_{12}'-\frac{m_4}{m_{34}}y_{34}'\right)-E. \quad \text{(A13)}$$

Next put $x'$ and $y_{12}'$ on the same footing, by defining new coordinates and masses,

$$\bar{x}=(m_{12}/m_1)x'-y_{12}^0-\bar{\gamma}y_{34}^0, \qquad \bar{\mu}_{12,34}=(m_1^2/m_{12}^2)\mu_{12,34},$$
$$\bar{\gamma}=m_{12}m_4/m_1m_{34},$$
$$\bar{y}_{12}=y_{12}'-y_{12}^0, \qquad \mu_{12},$$
$$\bar{y}_{34}=y_{34}'-y_{34}^0, \qquad \mu_{34}. \quad \text{(A14)}$$

The potential terms in $H-E$ become

$$\bar{V}_{12}(\bar{y}_{12})+\bar{V}_{34}(\bar{y}_{34})+\bar{V}_I(\bar{x}-\bar{y}_{12}-\gamma\bar{y}_{34})=V_{12}(\bar{y}_{12}+y_{12}^0)$$
$$+V_{34}(\bar{y}_{34}+y_{34}^0)+V_I[(m_1/m_{12})(\bar{x}-\bar{y}-\bar{\gamma}\bar{y}_{34})]. \quad \text{(A15)}$$

The operator is finally made dimensionless by dividing by $\hbar\omega_{12}$ and absorbing dimensional factors into the second differential operators. Define

$$x=(\mu_{12}\omega_{12}/\hbar)^{1/2}\bar{x},$$
$$y_{12}=(\mu_{12}\omega_{12}/\hbar)^{1/2}\bar{y}_{12},$$
$$y_{34}=(\mu_{34}\omega_{34}/\hbar)^{1/2}\bar{y}_{34},$$
$$\bar{\mu}=\mu_{12,34}'/\mu_{12}=m_1m_{34}/Mm_2,$$
$$\gamma=(m_2/m_3)(\mu_{34}\omega_{12}/\mu_{12}\omega_{34})^{1/2} \quad \text{(A16)}$$

to obtain the generalization of Eq. (19),

$$H-E=-(1/2\mu)(\partial^2/\partial x^2)-\tfrac{1}{2}(\partial^2/\partial y_{12}^2)$$
$$-(\omega_{34}/\omega_{12})(\partial^2/\partial y_{34}^2)+V_{12}'(y_{12})+V_{34}'(y_{34})$$
$$+V_I'(x-y_{12}-\gamma y_{34}). \quad \text{(A17)}$$

The potentials are related to their original forms by

$$V_{12}'(y_{12})=V_{12}[(\hbar/\mu_{12}\omega_{12})^{1/2}y_{12}+y_{12}^0]/\hbar\omega_{12},$$
$$V_{34}'(y_{34})=V_{34}[(\hbar/\mu_{34}\omega_{34})^{1/2}y_{34}+y_{34}^0]/\hbar\omega_{12},$$
$$V_I'(x-y_{12}-\gamma y_{34})$$
$$=V_I[(m_1/m_{12})(\hbar/\mu_{12}\omega_{12})^{1/2}(x-y_{12}-\gamma y_{34})]/\hbar\omega_{12}. \quad \text{(A18)}$$

* National Science Foundation Predoctoral Fellow, 1966–1969.
† Contribution No. 3909.
‡ Presently at the Department of Chemistry, Purdue University, Lafayette, Ind. 47907.

[1] M. E. Riley, thesis, California Institute of Technology, 1968 (unpublished); M. E. Riley and A. Kuppermann, Chem. Phys. Letters **1**, 537 (1968).
[2] S-K Chan, J. C. Light, and J. Lin, J. Chem. Phys. **49**, 86 (1968).
[3] D. Secrest and B. R. Johnson, J. Chem. Phys. **45**, 4556 (1966). For earlier work in multichannel invariant imbedding consult F. Calogero, *Variable Phase Approach to Potential Scattering* (Academic Press Inc., New York, 1967), Chap. 19.
[4] R. Gordon, J. Chem. Phys. **51**, 4 (1969).
[5] A. Cheung and D. Wilson, J. Chem. Phys. **51**, 4733 (1969).
[6] (a) A. B. Bhatia, *Ultrasonic Absorption* (Oxford University Press, 1967), for values of $\epsilon$ and $\sigma$; (b) G. Herzberg, *Spectra of Diatomic Molecules* (D. Van Nostrand, Co., Inc., Princeton, N.J., 1939), for values of $D_e$ and $\beta$; (c) K. F. Herzfeld and T. A. Litovitz, *Absorption and Dispersion of Ultrasonic Waves* (Academic Press Inc., New York, 1959).
[7] K. E. Shuler and R. Zwanzig, J. Chem. Phys. **33**, 1778 (1960).
[8] D. Rapp and T. E. Sharp, J. Chem. Phys. **38**, 2641 (1963).
[9] In HOLJ computations, 90%–95% of the net computing time was spent in calculating the potential matrix elements $V_{mn}(x)$ and only 5%–10% on actual solution of the CC equations. In HOEXP calculations, only about 1%–2% of the time was spent computing potential matrix elements. Similar percentage figures would hold even for the CC integration techniques of Refs. 4 and 5.